Int. J. Heat Mass Transfer. Vol. 37, No. 1, pp. 69–80, 1994
Printed in Great Britain

0017–9310/94 $6.00+0.00

A phenomenological model for boiling heat transfer and the critical heat flux in tubes containing twisted tapes

J. WEISMAN, J. Y. YANG† and S. USMAN
Nuclear Engineering Program, University of Cincinnati, Cincinnati, OH 45221, U.S.A.

(*Received* 25 *January* 1993 *and in final form* 14 *June* 1993)

Abstract—New critical heat flux (CHF) and boiling heat transfer data were obtained in the subcooled and low quality regions using refrigerant 113. These data were obtained in a 0.61 cm round tube containing a twisted tape having a twist ratio of 6.25. The new CHF data, plus water data from the literature, were compared to a modified version of the CHF predictive model based on bubble crowding and coalescence in the bubbly layer [Weisman and Pei, *Int. J. Heat Mass Transfer* **26**, 1463–1478 (1983), Weisman and Illeslamlou, *Fusion Tech.* **13**, 654–659 (1988)]. Reasonably good predictions were obtained within the range of the model. It was also found that the Yang and Weisman [*Int. J. Multiphase Flow* **17**, 77–94 (1991)] extension of the CHF model to boiling heat transfer held for swirling flow.

INTRODUCTION

DEVICES which can augment heat transfer are now finding application in a variety of situations. One approach to heat transfer augmentation is the insertion of a twisted tape inside the tube carrying the coolant. This device is particularly useful in boiling heat transfer where the swirling flow produced by the tape leads to a substantial increase in CHF. In view of the interest in using subcooled boiling in tubes for cooling of fusion reactor components [1, 2], it was believed that a further investigation of this phenomenon would be useful.

In addition to providing insight into swirl flow behavior, we wished to determine whether the CHF prediction procedure of Weisman *et al.* [3, 4], could be extended to swirl flow behavior. Successful application of this predictive procedure would provide further evidence that the Weisman *et al.* model appropriately describes flow-boiling CHF at subcooled and low-quality conditions.

PREVIOUS CHF STUDIES USING INTERNAL TWISTED TAPES

Swirl flow critical heat flux data with low pressures were first obtained by Gambill *et al.* [5], Drizius *et al.* [6] and Rosuel and Sourioux [7]. Unfortunately, all of the Rosuel and Sourioux data were obtained at void fractions above the range of the Pei–Weisman [3] model.

More recent low-pressure subcooled data, obtained for fusion reactor applications [8, 9], are also largely below the pressure range of Pei–Weisman model (for water, $P > 6.5$ bar). Only one point from Inasaka *et al.* [8] could be considered. Additional data were obtained by Koski and Croessmann [10] but only one side of the tube was heated and therefore these data were deemed unsuitable.

Critical heat flux data were obtained at elevated pressures by a number of investigators but only some of these studies [11–16] contained enough information to allow analysis. Of those with sufficient information, only the data of Viskanta [15] and Henkel *et al.* [16] had any significant number of points in the void fraction range ($\langle\alpha\rangle < 0.8$) of the Pei–Weisman model.

The only twisted-tape CHF data for a fluid other than water were those of Staub [13] and Gambill and Bundy [17]. However, all of Staub's R-22 data were at void-fractions above the range of the Pei–Weisman model. Although the ethylene glycol data of Gambill and Bundy [17] were within the void range of the Pei–Weisman model, the basic model had never been shown applicable to ethylene glycol. Therefore, these data were not considered useful for present purposes.

Empirical correlations for subcooled or low quality twisted-tape CHF have been developed by several investigators [5, 6, 8, 18, 19]. Jensen [20] appears to be the only investigator who devised a general correlation for twisted-tape CHF for flow with significant exit qualities. Since none of the previous correlations were based in on a real phenomenological model of swirl flow behavior, development of such a model appeared appropriate.

At the outset of this study, there appeared to be sufficient swirl-flow CHF data to test a modification of the Pei–Weisman model against water behavior. It appeared that some of the low-pressure data of refs. [5, 6, 8], and some of the high pressure data of refs. [15, 16], would provide a sufficient data base. However, no suitable data for a fluid other than water was available.

†Present address: Primary Fluid Systems Department, KAERI, P.O. Box 7, Dae-Duk Danji, Taejon, Korea.

NOMENCLATURE

a two phase multiplier in turbulent intensity equation
b empirical constant (set at 2.5)
c_p specific heat [J kg^{-1} K^{-1}]
D tube diameter [m]
De equivalent diameter, (4 × area/perimeter) [m]
D_h 2 × hydraulic radius [m]
d_b, d_H bubble diameter at departure and from equation (20), respectively [m]
d_L bubble diameter computed from Levy's departure criterion [m]
d_R average diameter of bubble after release into core fluid [m]
f friction factor
G total axial mass flux based on empty tube area [kg m^{-2} s^{-1}]
G' lateral mass velocity from core to bubbly layer due to turbulence [kg m^{-2} s^{-1}]
G_c mass velocity at which dispersed flow occurs [kg m^{-2} s^{-1}]
g, g_0 acceleration and gravitational acceleration [m s^{-2}]
g_{acc} acceleration due to swirl [m s^{-2}]
g_c gravitational conversion factor [(mass-length)/(force)(time^2)]
h_1, h_2 enthalpy of core fluid and bubbly layer mixture, respectively [J kg^{-1}]
h_f saturated liquid enthalpy [J kg^{-1}]
h_{fg} enthalpy change on evaporation [J kg^{-1}]
h_l, h_{bl} enthalpy of liquid and enthalpy of liquid at point of bubble detachment, respectively [J kg^{-1}]
i_b turbulent intensity at bubbly layer core interface
k, K, K_1 constants
L test section length [m]
l_c Prandtl mixing length [m]
M mass
P power [W]
Pr_l Prandtl number for liquid phase
P_H heated perimeter [m]
q'', q''_{CHF} total heat flux and CHF heat flux, respectively [W m^{-2}]
q''_b heat flux effective in generating vapor [W m^{-2}]
q''_i heat flux based on entire test section length [W m^{-2}]
r, r_0 radial position and outer radius of tube, respectively [m]
R (predicted critical heat flux)/(measured critical heat flux)
Re Reynolds number, DG/μ_{avg}
U^* frictional velocity [m s^{-1}]
u_t terminal settling velocity of bubble [m s^{-1}]
v_{vg} radial velocity created by vapor generation, $q''_b/(\rho_g h_{fg})$ [m s^{-1}]
v', $\bar{v}'$ radial fluctuating velocity and mean value of v', respectively [m s^{-1}]
$\sqrt{(\overline{v'^2})}$ root mean square value of v'
x_1, x_2 average quality in core region and bubbly layer, respectively
$x_{1,L}$, $x_{1,L-z}$ core quality computed at distance L and $(L-z)$ from entrance, respectively
y (axial distance for 180° twist)/D
z axial distance from point of bubble release [m].

Greek symbols
α_1, α_2 average void fraction in core and bubbly layer, respectively
$\langle\alpha\rangle$ average void fraction (across entire cross section)
ΔT_{sat} wall temperature-saturation temperature [K]
μ_l, μ_{avg} viscosity of liquid and mixture, respectively [kg m^{-1} s^{-1}]
$\mu(R)$ mean value of R
ρ_l liquid density at bulk temperature [kg m^{-3}]
ρ_g vapor density [kg m^{-3}]
$\bar{\rho}$ average density of fluid [kg m^{-3}]
σ surface tension [N m^{-1}]
$\sigma_{v'}$ standard deviation of v', $(G/\bar{\rho})i_b$
$\sigma(R)$ standard deviation of R
τ_w shear stress at wall [N m^{-2}]
Ψ parameter defined by equation (11)
ω angular velocity [rad s^{-1}].

TEST AND ANALYSIS PROGRAM

To obtain swirl-flow boiling heat transfer and CHF data with a fluid other than water, experiments were conducted using the University of Cincinnati's boiling refrigerant loop. This apparatus was described previously by Crawford *et al.* [21]. Further, the apparatus modifications and procedures used to gather boiling and CHF data were described in some detail by Yang and Weisman [22].

The heat transfer test section, heated by direct passage of AC current, provided a uniform heat flux in the test region. It was basically the same as used for previous tests and consisted of a 42 cm length of Inconel 600 tubing which originally had an o.d. of 0.95 cm (3/8") and an i.d. of

0.62 cm. The central 29 cm of the test section had its outer diameter machined down to 0.72 cm, giving a wall thickness of 0.051 cm. The tube was welded to an Inconel 600 flange at both ends. Current-carrying cables were attached to Inconel tabs which were part of the flanges. The flanges were insulated from the loop.

Tests were conducted using R-113 at a pressure of 0.79 MPa. This pressure was used as it was within the capabilities of the circulating loop yet sufficiently high so that substantial inlet subcooling could be obtained. CHF values were determined as a function of mass flux and inlet subcooling. Mass fluxes ranged from approximately 2.2×10^6 to 12×10^6 kg m^{-2} h^{-1} and inlet subcooling from 88 to 29°C. Boiling heat transfer coefficients were determined over a similar range. Measurement uncertainties may be obtained from Yang [23].

The present experiments were preceded by CHF and boiling heat transfer tests carried out in round tube test sections without any inserts [22]. The good agreement of the empty tube data with predictions in the dispersed flow region indicated the adequacy of the experimental arrangement. In the present study, the test section contained a 0.13 mm thick nichrome tape twisted so that a 180 degree turn was made every 3.8 cm. Hence, the twist ratio, y, for this test is 6.25. The tape width was such that the tape fitted tightly against the tube walls.

As the nichrome tape was in direct contact with the electrically-heated tube, some current must have been carried by the tape. However, since the cross sectional area of the tape was very much smaller than that of the tube, and the Nichrome had a slightly higher resistivity than the Inconel, only a small fraction of the total current was carried by the tape. Computations indicated that the tape current was less than 5% of the total current.

Boiling heat transfer experiments were conducted by setting the pressure and inlet temperature and then gradually increasing the heat flux in a stepwise manner. The test section temperature was determined by reading the upper thermocouple on the outer wall of the test section. A signal conditioner removed the AC portion of the thermocouple signal and amplified the DC output so that it could be read on a digital voltmeter. The inner wall temperature was determined by subtracting the calculated temperature difference across the tube wall.

Critical heat flux measurements were conducted in a similar manner. The heat flux was very slowly increased until a rapid temperature rise in the exit thermocouple indicated that the critical heat flux was reached.

RESULTS OF EXPERIMENTAL PROGRAM

The critical heat flux tests resulted in 58 valid data points at four different mass fluxes. A complete listing of these data may be obtained from Yang [23]. The most comprehensive data were taken at mass fluxes of approximately 4.9×10^6 and 9.8×10^6 kg m^{-2} h^{-1}. These data are plotted against the enthalpy of the fluid at the CHF location in Figs. 1(a) and (b). Also shown are the CHF data taken at the same velocities in the empty-tube test section. As expected, the presence of the twisted tape provides a significant enhancement in the observed critical heat flux. The enhancement appears to be somewhat greater at the highest enthalpies. The scatter seen is typical of CHF data.

The initial boiling heat transfer tests produced a saturated mixture of vapor and liquid at the test section exit. In contrast with the data previously obtained with an empty tube [22], where a single saturated-boiling curve was obtained, there appears to be a separate saturated boiling curve for each mass flux (see Fig. 2). Further, the curves all lie above the saturated boiling curve obtained with the empty tube (curve also shown in Fig. 2) as the mass flux is decreased, the data tend toward the empty-tube curve.

The increased heat flux observed for a given wall temperature is readily explainable by the effect of the increased acceleration produced by swirling flow. If we assume that the saturated flow boiling curve will behave similarly to flow boiling in an empty tube, data trends may be predicted using a pool boiling correlation which includes gravitational acceleration. The widely used pool boiling correlation of Rohsenow [24] has the form

$$\frac{C_p\Delta T_{sat}}{h_{fg}P_{r_l}^{0.7}}=C_{sf}\left[\frac{q''_b}{\mu_l h_{fg}}\sqrt{\left(\frac{g_c\sigma}{g(\rho_l-\rho_g)}\right)}\right]^{1/3} \tag{1}$$

where C_{sf} is a constant. For a given fluid and surface at a fixed pressure,

$$\Delta T_{sat}=C'[q''_b\sqrt{(C''g_c/g)}]^{1/3} \tag{2}$$

where C' and C'' are constants. At a given heat flux, it follows that

$$\Delta T_{sat}=C'''(g_c/g)^{1/6}. \tag{3}$$

If we compare the values of ΔT_{sat} at an acceleration g to the ΔT_{sat} observed when $g=g_0$, where g_0 is the acceleration due to gravity, we have

$$(\Delta T_{sat})_g/(\Delta T_{sat})_{g_0}=(g_0/g)^{1/6}. \tag{4}$$

The force acting on a bubble is the resultant of the vertical gravitational force and the radial force due to the swirling flow. Since acceleration is proportioned to force, the effective 'gravity', g_{eff}, acting on the vapor bubbles generated at the heater surface, is given by the vector addition of the radial and gravitational acceleration. This yields

$$g_{eff}=\sqrt{(g_{acc}^2+g_0^2)}. \tag{5}$$

The value of g_{acc} is determined from [24]

$$g_{acc}=\frac{4.96}{D}\left(\frac{G}{\rho_l y}\right)^2. \tag{6}$$

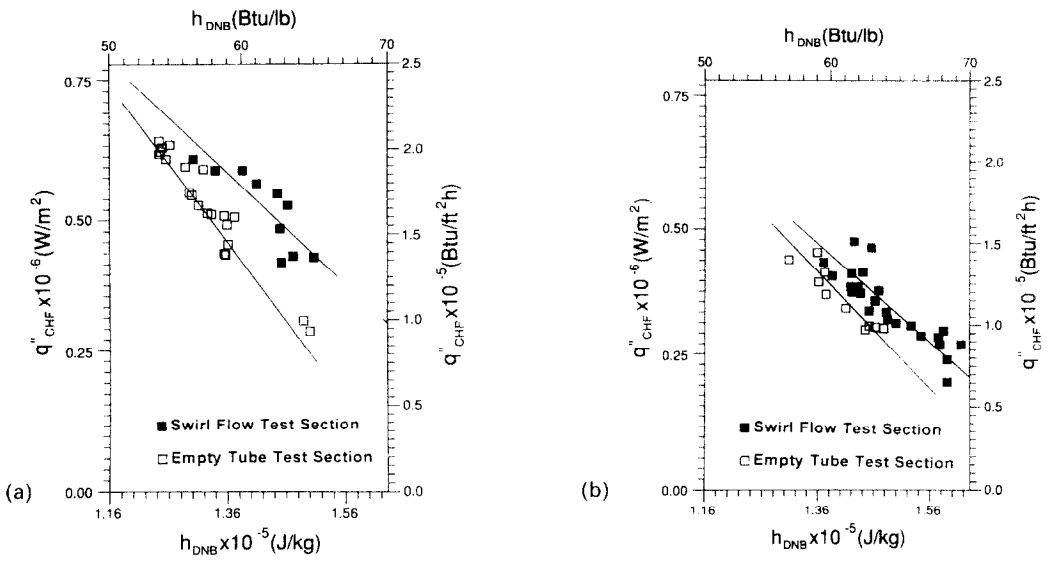

FIG. 1. Comparison of CHF data in the presence of a twisted tape with empty tube data: (a) $G = 9.45$–10.35×10^6 kg m^{-2} h^{-1}; (b) $G = 4.85$–5.05×10^6 kg m^{-2} h^{-1}.

By using equations (4)–(6), the curves for the mass fluxes used in Fig. 2 were determined using the empty tube boiling curve for $(\Delta T_{sat})_{q_0}$ at a given flux. These predictions, shown in Fig. 2, are in good agreement with the data.

The subcooled boiling data were obtained with both inlet temperature and mass flux held constant. (See Figs. 5(a) and (b) for typical data.) The subcooled boiling curves show the same general trends as seen in the previous studies in an empty tube [21]. Just as in the earlier tests, the heat flux increases with both increasing mass velocity and inlet subcooling for a given wall temperature. As the exit liquid approaches saturation, the subcooled boiling curves approach the saturated boiling curves. However, the heat fluxes obtained at a given wall temperature were significantly above the fluxes obtained with an empty tube.

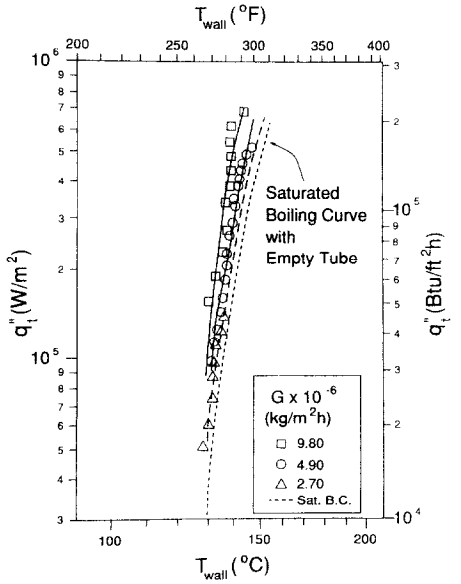

FIG. 2. Saturated boiling heat transfer rates in the presence of a twisted tape.

The wall heat fluxes were computed from the test section power without making any allowance for the small current carried by the twisted tape. In part, this was done because it was difficult to ascertain the degree of electrical contact between the tube and the tape and only an upper limit for the current carried by the tape could be determined. Further, it appears that previous investigators using electrically heated walls also ignored [5, 6, 15] the tape current. CHF data computed in this manner are therefore consistent with the literature data. In addition, in any practical application of twisted tapes in a heat exchanger, the tape would be acting as a fin and dissipating some heat. The tube would then be capable of dissipating more heat that computed using the actual CHF value and the area of the tube alone. Since the total error was clearly less than 5%, the approach was considered acceptable.

PHENOMENOLOGICAL MODEL OF CHF IN AN EMPTY TUBE

The modelling of the subcooled and low quality swirl flow behavior proposed herein is based on the phenomenological model of Weisman and Pei [3] and its subsequent extensions [4, 25]. The model assumes that the critical heat flux is governed by the behavior of the bubbly layer adjacent to the heated surface. The outer edge of the bubbly layer is located where the eddy size has become large enough to influence the

bubbles. It is assumed that the turbulent interchange at the bubbly layer edge limits the rate of heat transfer.

Weisman and Pei [3] expressed the turbulent interchange at the bubbly layer edge in terms of a mass balance which they wrote as

$$G'(x_2-x_1) = q''_b/h_{fg} = \frac{(h_f-h_{id})}{(h_i-h_{id})}(q''/h_{fg}). \quad (7)$$

In dimensionless form, this becomes

$$q''_{CHF}/(h_{fg}G') = (x_2-x_1)\frac{(h_f-h_{id})}{(h_i-h_{id})}. \quad (8)$$

The quantities x_1 and x_2 represent the actual vapor qualities in the core region and bubbly layer, respectively, at CHF. The quality x_2 corresponds to the maximum void fraction that is possible in a bubbly layer of independent, slightly distorted, ellipsoidal bubbles just prior to agglomeration ($\alpha_2 = 0.82$). At high mass fluxes, x_2 is related to α_2 by assuming homogeneous flow.

The quantity G', representing the mass flow rate into the bubbly layer, is determined by the turbulent velocity fluctuations at the bubbly layer edge. The fraction of the turbulent velocity fluctuations which reach the wall are those in which the velocity exceeds the average vapor velocity away from the wall. At the bubbly layer–core interface, the effective mass flux toward the wall is

$$G' = \Psi i_b G, \quad (9)$$

where G is the total axial mass flux. The product $i_b G$ represents the flux toward the wall in the absence of outward flow. The parameter i_b, representing the turbulent intensity at the bubbly layer–core interface, is calculated as the product of the single-phase turbulent intensity at the bubbly layer edge and a two-phase enhancement factor. This results in

$$i_b = 0.462(k')^{0.6}(Re)^{-0.1}(d_b/D)^{0.6}[1+a(\rho_l-\rho_g)/\rho_g], \quad (10)$$

where the empirical coefficients are given by

$$a = a_0, \quad G \leqslant 9.7\times10^6 \text{ kg m}^{-2}\text{ h}^{-1}$$

$$a = a_0(G/9.7\times10^{-6})^{-0.3} G > 9.7\times10^6 \text{ kg h}^{-1}\text{ m}^{-2}$$

$$a_0 = 0.135, \quad k' = 2.5.$$

By assuming the velocity fluctuations are normally distributed, the parameter Ψ, which represents the fraction of the velocity fluctuations effective in reaching the wall, was found to be

$$\Psi = \frac{1}{\sqrt{(2\pi)}}\exp[-\tfrac{1}{2}(v_{11}/\sigma_{v'})^2] - (\tfrac{1}{2})(v_{11}/\sigma_{v'})\operatorname{erfc}[v_{11}/(\sigma_{v'}\sqrt{(2)})]. \quad (11)$$

Ying and Weisman [25] examined higher qualities and lower velocities than those originally considered. They extended the model's range by recognizing that, at void fractions above 0.64, the quality of the core fluid adjacent to the bubbly layer is below the core average quality. Therefore, when $\alpha > 0.64$, x_1 in equation (8) is replaced by $(x_1)_{eff}$, which is appropriately below x_1. In addition, it is necessary to increase 'a' at low mass velocities.

More recently, Weisman and Illeslamlou [4] considered the highly subcooled region where the original predictive procedure tended to overpredict the available data somewhat. They concluded that the overpredictions were the result of using equation (7) to predict the boiling heat flux in a region where the liquid enthalpy h_l was close to the enthalpy of bubble detachment h_{id}. To avoid this difficulty, they computed CHF from a bubbly layer energy balance,

$$q''_{CHF} = G\Psi i_b(h_2-h_1). \quad (12)$$

The fraction of the total energy going to produce vapor was obtained by simultaneous solution of the energy balance (equation (12)) and a mass balance. This allows determination of v_{11} and hence enables the computation of Ψ. With these revisions, they were able to satisfactorily predict highly subcooled DNB for water, refrigerant 113, and liquid nitrogen. They suggested that this procedure should be used whenever the thermodynamic equilibrium quality is below -0.12.

Before extending the previous model to swirl flow, the refrigerant 113 data obtained in the empty tube test section were reexamined. It was observed that, while good predictions were obtained at higher mass fluxes, predictions deviated from observations at the lower mass fluxes. The deviation began where the low velocity correction was applied to the parameter 'a' in the two-phase turbulent intensity multiplier. Upon closer examination, it was determined that, when Ying and Weisman [25] obtained this correction, they only had water and helium data to consider. On the basis of these data, they suggested a correction based on the velocity of the entering liquid. However, the available low velocity range refrigerant 113 data do not appear to fit the previous pattern. An improved low velocity correction for 'a' was therefore sought.

In correlating CHF data from horizontal tubes, Wong *et al.* [26] corrected the prediction obtained at mass fluxes below the onset of dispersed bubble flow by an amount which depended on the ratio of the observed mass flux to the mass flux at the onset of dispersed flow, G_c. To see whether this approach would satisfactorily explain the observed behavior, R, the ratio of predicted to measured CHF, was plotted vs G/G_c. These predictions were obtained with the parameter 'a' being held constant at the value of 0.135. The value of G_c is obtained from the criterion of Weisman *et al.* [27]. In simplified form, this is:

$$(G_c/\rho_L) = 2.75\,(\text{m s}^{-1})\left(\frac{\rho_{SL}}{\rho_L}\right)^{0.33}\left(\frac{D}{D_s}\right)^{0.16} \times \left(\frac{\mu_{SL}}{\mu_L}\right)^{0.09}\left(\frac{\sigma_L}{\sigma_{SL}}\right)^{0.24} \quad (13)$$

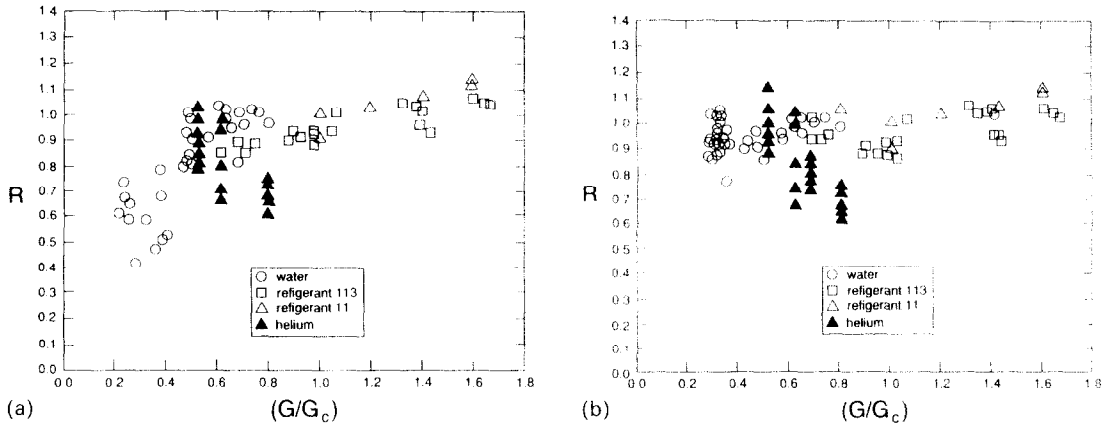

FIG. 3. Comparison of predicted and measured CHF in empty tubes: (a) without low mass flux correction; (b) with revised low mass flux correlation.

where the subscript 'SL' indicates properties of water at 20°C and one bar and 'L' indicates the properties of liquid being considered. The parameter D_s indicates a 2.54 cm diameter. The result is shown in Fig. 3(a). While there is significant scatter, all of the data now show the same trend. Although the He data were taken at low mass fluxes, the very low surface tension of He leads to a low value of G_c and hence the data roughly conform to the general trend.

Generally, good agreement between the refrigerant 113 and water data was obtained using the following expression for 'a'

$$a = a_0 + 1.51(1 - G/G_c)^2 - 0.25(1 - G/G_c) \tag{14}$$

where a_0 has the value (0.135) used in equation (10). The results of this approach are shown in Fig. 3(b) where the ratio of predicted to observed heat flux, R, is plotted against the ratio (G/G_c). Although the helium data still show appreciable scatter, they are in the correct range. Equation (14) was therefore used to calculate 'a' in the swirl flow analysis whenever $G < G_c$. At higher values of G, the expressions following equation (10) were used.

EXTENSION OF PHENOMENOLOGICAL MODEL ANALYSES OF SWIRL FLOW CHF

The proposed model is based on the assumption that the vapor bubbles in the bubbly layer are so small that the radial force acting on them at the bubbly layer edge is negligible in comparison with the forces imposed by the turbulent eddies. If this assumption is correct, CHF conditions with substantially subcooled liquid should be predicted by the same model used for empty tubes providing both the bubble diameter and turbulent intensity are revised.

Weisman and Pei [3] computed the diameter of the bubbles in the bubbly layer using Levy's approach [28]. The bubble diameter, d_b, was obtained by a balance between surface tension and frictional forces when $G > 3.5 \times 10^6$ kg m^{-2} h^{-1} and buoyant forces are small in comparison with frictional drag. For swirling flow, we must consider the radial force on the bubbles produced by the swirl in addition to frictional drag. However, the frictional drag and inward centrifugal force are not in the same direction. If we ignore the vertical buoyant force, the resultant force is given by the root mean square of the radial and drag forces. By proceeding in a manner similar to that of Levy [28], the force balance for a bubble on the wall at the point of departure is:

$$\left\{\left[C_a \frac{g_{acc}}{g_c}(\rho_l - \rho_g) d_b^3\right]^2 + \left[C_f \frac{\tau_w}{D_H} d_b^3\right]^2\right\}^{1/2} = C_s d_b \sigma. \tag{15}$$

The first term on the left represents the inward radial force with g_{acc} being computed via equation (6). It has the same form as Levy's buoyancy term but g_{acc} replaces the acceleration of gravity. The second term on the left represents the frictional force and the right hand term represents the surface tension force. Upon combining constants and rearranging terms, we have

$$d_b = \frac{C_1 \sigma}{\{[C_2(g_{acc}/g_c)(\rho_l - \rho_g)]^2 + (\tau_w/D_h)^2\}^{1/4}} \tag{16}$$

Since constants have been combined in the same manner as used by [28] and [25], we take C_1 equal to its previous value and set C_2 as equal to the constant found appropriate for the buoyancy term. We therefore have $C_1 = 0.015$ and $C_2 = 0.1$.

The neglect of the buoyancy force in equation (15) is justified only as long as this force is small with respect to the frictional drag. The higher friction factors in tubes with twisted tapes allows this assumption to be used over a wider velocity range than was possible in straight tubes. Based on the Weisman and Pei lower velocity limit of 3.5×10^6 kg m^{-2} h^{-1} it was estimated that the approach taken here should hold down to flows of about 2.5×10^6 kg m^{-2} h^{-1}.

We shall assume that the turbulent intensity in a tube containing a twisted tape follows the same general relationship that holds in an empty round tube. Weisman and Pei [3] showed, for an empty tube, i_b at the bubbly layer edge is

$$i_b = K_1 \left(\frac{\bar{\rho}}{G}\right)\sqrt{\left(\frac{\tau_w g_c}{\bar{\rho}}\right)}\left(\frac{k d_b}{De}\right)^{0.6}\left[a\left(\frac{\rho_l-\rho_g}{\rho_g}\right)+1\right]. \tag{17}$$

Therefore, for a given mass flux and density, the ratio of the turbulent intensity with swirling flow to that in an empty tube is

$$i''_{b}/i_{b,\text{empty}} = \left(\frac{\tau_{w,\text{swirl}}}{\tau_{w,\text{empty}}}\right)^{1/2}\left(\frac{d_{b,\text{swirl}}}{d_{b,\text{empty}}}\right)^{0.6}\left(\frac{D_{e,\text{empty}}}{D_{e,\text{swirl}}}\right)^{0.6} \tag{18}$$

if the two-phase enhancement factor $[1+a(\rho_l-\rho_g)/\rho_g]$ remains constant. The ratio was evaluated by: (a) noting that for a tape of negligible thickness the ratio $(De_{\text{empty}}/De_{\text{swirl}})$ is $(1+2/\pi)$, (b) obtaining the value of $(\tau_w)_{\text{swirl}}$ via the empirical friction factor correlation of Manglik and Bergles [29] for tubes with a twisted tape. We then obtain the following:

$$i''_{b}/i_{b,\text{empty}} = \left(1+\frac{2.752}{y^{1.29}}\right)^{1/2}\left(1+\frac{2}{\pi}\right)^{0.725}\left(\frac{d_{b,\text{swirl}}}{d_{b,\text{empty}}}\right)^{0.6}. \tag{19}$$

If all of the foregoing assumptions hold, subcooled CHF in the presence of twisted tapes should be predicted by using the modified bubble diameter and turbulent intensity along with the previously developed prediction procedure. However, in saturated boiling the effect of the swirling flow in reducing the vapor fraction in the fluid adjacent to the bubble layer must be considered.

The bubble diameters at departure from the wall, computed via equation (16), for conditions typical of the available swirl flow data were very small. In fact, the bubble departure diameters were sufficiently small so that the released bubbles would be carried with the turbulent eddies. However, once the bubbles escape into the core liquid, they may be expected to agglomerate and grow. Studies of bubbles in empty tubes show that this agglomeration proceeds until the rate of agglomeration and rate of breakup are in equilibrium. Previous studies [30] indicate that the bubbles approach d_H, the equilibrium diameter reported by Hinze [31], which is much larger than d_b. The value of d_H is computed from

$$0.725 = [\rho_l^3(P/M)^2/(g_c\sigma^3)]^{1/5} d_H. \tag{20}$$

In their study of the effect of boiling on flow patterns, Weisman and Du [32] concluded that the average diameter, d_R, of bubbles released from a heated surface increased with distance from the release point. They concluded

$$d_R = d_L\, e^{-Kz/De} + d_H(1-e^{-Kz/De}) \tag{21}$$

where d_L was computed from Levy's bubble diameter equation [28] and d_H from equation (20). They suggested that $K = 0.035$.

It is assumed that the bubbles released from the heated surface grow in accordance with equation (21). They are assumed to remain in the core fluid until they have grown to a size such that the radial velocity exceeds the r.m.s. turbulent fluctuating velocity, $\sqrt{\overline{v'^2}}$. At that point, they are considered to be rapidly carried to the center of the tube. The only bubbles in the core region are therefore those which are small enough to be carried by the turbulent eddies.

The foregoing postulates that bubbles move to the tube center when

$$(u_T) = b\sqrt{\overline{v'^2}}. \tag{22}$$

The small size bubbles will follow Stokes law providing the gravitational acceleration is replaced by the radial acceleration. Hence,

$$u_T = \frac{\omega^2(D/2)(\rho_l-\rho_g)d_R^2}{18\mu_l} = C_T d_R^2 \tag{23}$$

or

$$d_R = \left(\frac{b\sqrt{\overline{v'^2}}}{C_T}\right) \tag{24}$$

since the $d_H \gg d_L$, we may approximate d_R by $d_H(1-e^{-Kz/De})$ and hence

$$\left(\frac{b\sqrt{\overline{v'^2}}}{C_T}\right)^{1/2} = d_H(1-e^{Kz/De}). \tag{25}$$

The distance, z, from the point of bubble release to where equation (25) is met is

$$z = -\frac{De}{K}\ln\left\{1-\frac{1}{d_H}\left(\frac{b\sqrt{\overline{v'^2}}}{C_T}\right)^{1/2}\right\} = -\frac{De}{K}\ln\left\{1-\left(\frac{b\sqrt{\overline{v'^2}}}{(u_T)_H}\right)^{1/2}\right\} \tag{26}$$

where $(u_T)_H$ is the value of u_T from equation (23) with d_R replaced by d_H.

The turbulent fluctuating velocity $\sqrt{\overline{v'^2}}$ in equation (26) is evaluated in the central region of the tube. For this region, Laufer's data [33] indicate that

$$\sqrt{(\overline{v'^2})}/U_\tau = 3.5 l_c/r_0. \tag{27}$$

In the central region of the core, (l_c/r_0) is independent of Reynolds number and is approximately 0.2. After replacing U_τ in terms of τ_w, we have for single phase conditions

$$\sqrt{\overline{v'^2}} = 0.7\sqrt{(\tau_w/\rho_l)}. \tag{28}$$

By using the usual relationship between τ and f, τ_w may be evaluated and the single-phase value of $\sqrt{\overline{v'^2}}$ can be determined. Yang and Weisman [22] concluded that the turbulent intensity, and hence $\sqrt{\overline{v'^2}}$, varied

with $[1+a(\alpha_s/0.82)^{2.5}(\rho_l-\rho_g)/\rho_g]$. Since the actual void fraction, α, in the region between the bubbly layer and vapor core is believed to be quite low, no two-phase correction was made to the value of $\sqrt{\overline{v'^2}}$ determined by equation (28).

The value of 'z' determined from equations (27) and (29) defines the region which provides the vapor to the fluid which is in contact with the bubbly layer. That is, the effective quality, x_{eff}, of fluid in contact with the bubbly layer is

$$x_{eff} = x_{(L)} - x_{(L-z)}. \quad (29)$$

The value of x_{eff} replaces x_1 in CHF computation (equation (8)) with saturated boiling.

COMPARISON OF PROPOSED MODEL WITH CHF DATA

Previous use of the Weisman–Pei model and its modifications, together with the low flow studies of this work, indicated that the model should be restricted to the following range:

$$0.0045 \leqslant (\rho_g/\rho_l) \leqslant 0.41 \quad \langle\alpha\rangle \leqslant 0.8$$

$$0.115 < D \leqslant 3.75\,\text{cm} \quad 3.5 \leqslant L \leqslant 365\,\text{cm}$$

$$0.3G_c \leqslant G \leqslant 144\times10^6\,\text{kg h}^{-1}\,\text{m}^{-2} \quad -0.47 \leqslant x_1.$$

When comparing the proposed model for swirl flow to available data, a slightly more restrictive range was used. We require $G > 2.5\times10^6$ kg m^{-2} h^{-1} so that equation (15) is valid. Since use of the model at $\alpha > 0.64$, required use of an empirical effective x_1 to account for a non-uniform distribution of voids, it was decided to limit consideration to $\alpha < 0.64$. The void distribution behavior in an empty tube is certainly not applicable to swirl flow conditions.

Initially, only the CHF data at subcooled conditions were considered [5, 6, 8, 15, 16]. In reviewing the data of Henkel *et al.* [16], it was observed that at a given mass flux, there was a sudden drop (step decrease) in the CHF as the quality was reduced. Henkel *et al.* [16] concluded that they had unstable flow conditions at low quality with their lower mass fluxes. It was assumed that these data represented premature CHF and, hence, should not be considered. Table 1 indicates the range of parameters examined for each of the data sets.

Before applying the modification developed for swirl flow, the subcooled swirl-flow data were compared to the unaltered Weisman–Illeslamlou (equation (12)) prediction [4], for empty round tubes. As expected, the mean of the predictions was below the data and a wide scatter (r.m.s. error $\simeq 19\%$) was observed.

The subcooled CHF data were then compared to the predictions using the Weisman–Illeslamlou form of the prediction procedure (equation (12)) with the turbulent intensity modified for swirl flow in accordance with the development of the previous section. Since the prediction procedure was used for slightly subcooled data, the value of x_1, the non-equilibrium quality in the core, was not set at zero but evaluated using the procedure of Weisman and Pei [3]. The results of this comparison are given in Table 2A, column A. It will be observed that $\mu(R)$ for the refrigerant 113 data ($\rho_g/\rho_l \approx 0.04$) is very close to one. The value of $\mu(R)$ for high pressure water data ($0.1 \leqslant \rho_g/\rho_l \leqslant 0.175$) is somewhat below 1 while $\mu(R)$ for the low pressure water data ($0.0045 \leqslant \rho_g/\rho_l \leqslant 0.019$) was well above 1.0.

In view of the foregoing, it was concluded that the density ratio term, which multiplies the single phase turbulent intensity, needed to be revised. There is no reason to assume that this empirical factor remains unchanged with swirl flow. For empty tubes this factor takes the form $\{1+a[(\rho_l-\rho_g)/\rho_g]\}$ with 'a' being a function of mass velocity. It was assumed that by modifying this multiplier to $\{1+ca[(\rho_l-\rho_g)/\rho_g]^n\}$ where 'c' and 'n' are constants, the observed pressure effect could be eliminated. It was found that, by setting $c = 1.5$ and $n = 0.9$, a significantly improved correlation could be obtained. The improved results are shown in column B of Table 2A. The refrigerant 113 and high pressure water data show $\mu(R)$ values close to unity and $\sigma(R)$ in the range of 0.05–0.085. The low pressure water data, however, still shows considerable scatter.

The predictions of the CHF data obtained under saturated boiling conditions were based on the original Pei–Weisman [1] model using a turbulent intensity appropriately modified for the effects of swirl flow and with the revised two-phase multiplier. The original Pei–Weisman model was chosen since it has received extensive validation for saturated boiling con-

Table 1. Parameter ranges for swirl flow CHF data

Investigator	Fluid	Pressure (bar)	Tube diameter (cm)	Test section length (cm)	r	Total no. of useful data pts	Mass flux (kg m^{-2} h^{-1})
Yang (present study)	Refrigerant 113	7.9	0.61	29	6.25	41	2.2–12×10^6
Gambill *et al.*	Water	6.6–37.5	0.52–0.9	14.8–44.2	2.3–12.0	8	28–98×10^6
Henkel *et al.*	Water	69.9–102.3	0.70	30	2.3–5.7	40	8.4–12.9×10^6
Drizius	Water	6.8–7.8	0.16	3.7–14.1	4.4–4.5	8	49–69×10^6
Viskanta	Water	138	0.79	45.7	5–10	30	2.4–9.8×10^6
Inasaka *et al.*	Water	7.0	0.6	10.0	3.9	1	19×10^6

Table 2. Statistical evaluation of CHF predictions

A—Subcooled CHF, prediction		A		B		C	
		Prediction with original two-phase turbulent intensity correction factor		Prediction with revised two-phase turbulent intensity correction factor		Prediction with revised two-phase correction factor & elimination of data with very high subcooling	
Data description	No. of data pts	$\mu(R)$	$\sigma(R)$	$\mu(R)$	$\sigma(R)$	$\mu(R)$	$\sigma(R)$
Water at low pressure (6.6–37.5 bar)	(Columns A & B) 17 (Column C) 14	1.12	0.30	1.10	0.29	1.00	0.18
Water at high pressure (69.9–138 bar)	9	0.84	0.082	0.99	0.085	0.99	0.085
Refrigerant 113 7.9 bar	29	0.97	0.052	0.99	0.049	0.99	0.049

B—Saturated boiling CHF predictions			
Data description	No. of data pts	$\mu(R)$	$\sigma(R)$
Water at high pressure (69.9–138 bar)	61	1.01	0.092
Refrigerant 113 (7.9 bar)	12	0.98	0.084
All saturated boiling data	73	1.00	0.091

ditions while the validation of the revised Weisman–Illeslamlou approach has been confined to subcooled conditions. Initially, no allowance was made for the reduction in x_1, the core fluid quality, due to the radial motion of the bubbles. As expected, the CHF conditions were underpredicted ($\mu(R) = 0.90$). To illustrate the opposite extreme, we then compared the data to predictions with x_1 arbitrarily set to zero. The expected overprediction of the CHF value was obtained ($\mu(R) = 1.09$).

Predictions of the saturated boiling CHF data obtained using an x_{eff}, determined using equation (29) and the developments of the previous section, were obtained for various values of the empirical constant 'b'. The best results were obtained with $b = 2.5$. With this value, good agreement was obtained between the predictions and the data ($\mu(R) = 1.00$ and $\sigma(R) = 0.085$) for all of the saturated boiling data. The statistical analysis of these data is given in Table 2B. The use of an effective core quality in CHF prediction appears to be successful.

To see if there were any significant trends with experimental conditions 'R' was plotted against a number of parameters (exit quality, (ρ_g/ρ_l), y, D, L and G). The only graph which showed a significant trend was the plot of R vs exit quality. The data scattered about a mean of one until high negative qualities (large subcooling) are encountered. At values of $\chi < -0.3$, predicted CHF values substantially exceed the measured values. It would appear that the present model does not apply at these high subcooling. If these very highly subcooled data points are eliminated, the statistical evaluation of 'R' is appreciably improved (see column C of Table 2A). The excluded points are probably in the attached bubble region where the present theory does not apply.

Figure 4 shows a parity plot of predicted CHF vs measured CHF which includes both saturated boiling CHF and subcooled CHF data. Data for CHF at thermodynamic qualities below (-0.3) have been omitted. As may be seen, the overall agreement between experimental data and predictions is generally good. It may also be observed that 92% of the

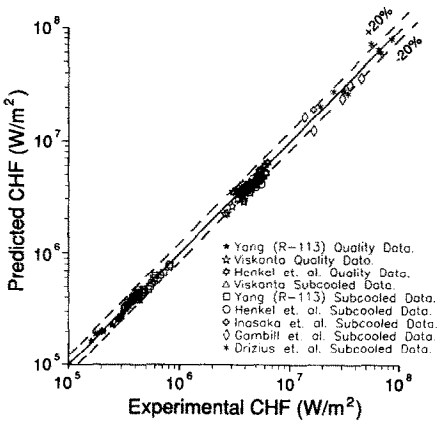

FIG. 4. Comparison of experimental and predicted CHF values in presence of twisted tape—all data for $\chi_{\text{CHF}} > -0.3$, $\alpha > 0.64$.

data lie within ±20% of the prediction. Statistical analysis, with all of the data considered as a single group, yields $\mu(R) = 1.0$ and $\sigma(R) = 0.097$ or a r.m.s. error of 9.7%. This compares quite favorably with empirical correlations of swirl flow CHF data. For example, Jensen [20] states that his empirical correlation showed an r.m.s. error of approximately 11.5% when compared to the quality CHF data available to him. In addition, the empirical correlations are restricted to being used with water only.

It was previously observed that the actual critical heat flux values for the R-113 data were slightly below those reported because a small current flowed through the twisted tape. If the maximum possible current flow is assumed to flow in the tape, the value of $\mu(R)$ for all the R-113 data would be increased from 0.99 to 1.04. The r.m.s. error for all data considered as a single group would be slightly increased because of the small rise in the overall mean.

EXTENSION OF MODEL TO PREDICTION OF NUCLEATE BOILING HEAT TRANSFER

Yang and Weisman [2] argued that, if the Weisman–Illeslamlou [4] formulation for subcooled CHF prediction is valid, the predictive approach should apply at heat fluxes somewhat below CHF. If this is so, equation (12) may be used to compute the value of the bubbly layer enthalpy. However, as noted previously, they concluded that the two-phase multiplier effect would vary with the bubbly layer void fraction. They therefore described the turbulent intensity by

$$i_b = 0.462(k)^{0.6} Re^{0.1} \left(\frac{d_b}{D}\right)^{0.6} \times \left[1 + \left(\frac{\alpha_2}{0.82}\right)^m a \frac{(\rho_l - \rho_g)}{\rho_g}\right]. \quad (30)$$

Once h_2 is determined from equation (12) using i_b from equation (30), then, F, the fraction of the heat flux producing boiling, is obtained from the simultaneous solution of equation (12) and the bubbly layer mass balance yielding

$$F = q''_b/q'' = h_{lg}(x_2 - x_1)/(h_2 - h_1). \quad (31)$$

The product (Fq'') is then the boiling heat flux and the predicted wall temperature is the temperature on the saturated boiling curve corresponding to this heat flux. By using this procedure, and with the empirical exponent $m = 2.5$, Yang and Weisman [22] were able to get good agreement between their boiling refrigerant 113 data and the predictions in empty round tubes.

The same approach has been used to obtain a prediction of the swirl flow subcooled boiling data obtained in this study. However, the equation for i_b has been modified to include the effect of the twisted tapes on the wall shear stress and to include the revised two-phase correction factor. The equation becomes

$$i_b = 0.462(k)^{0.6} Re_0^{0.1} \left(1 + \frac{2.752}{\text{[illegible]}}\right)^{\text{[illegible]}} \left(1 + \frac{2}{\pi}\right)^{\text{[illegible]}} \times \left(\frac{d_h}{D_e}\right)^{0.6} \left[1 + \left(\frac{\alpha_2}{0.82}\right)^m a \left(\frac{\rho_l - \rho_g}{\rho_g}\right)^{\text{[illegible]}}\right] \quad (32)$$

where De, the equivalent diameter, and Re_0, the Reynolds number, are based on the empty tube diameter but d_h refers to conditions with the twisted tape. Once the boiling heat flux has been determined via an iterative solution of equations (31) and (32), together with the

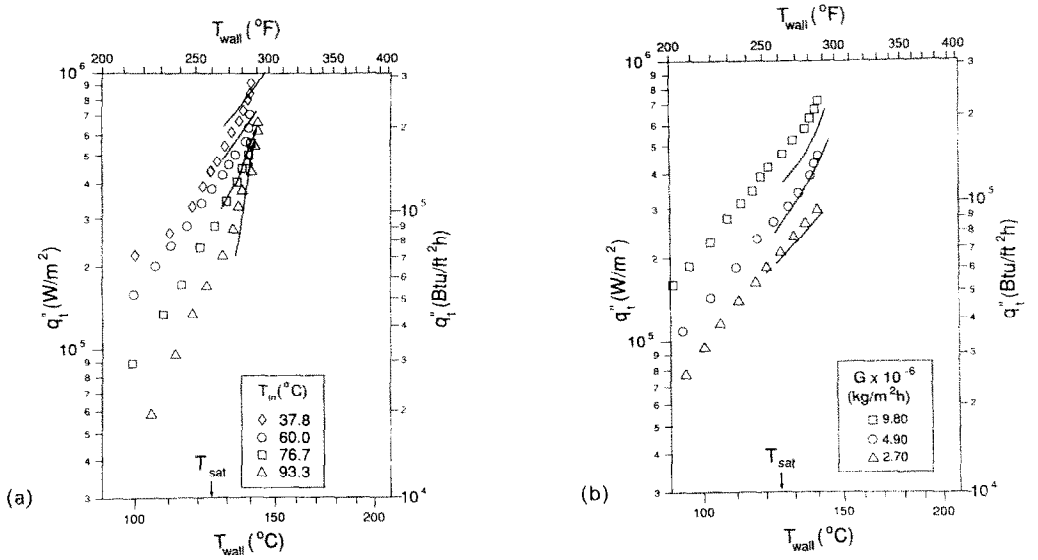

FIG. 5. Comparison of subcooled boiling heat transfer data with predictions ($P = 7.9$ bar): (a) effect of inlet subcooling ($G = 9.8 \times 10^6$ kg m^{-2} h^{-1}); (b) effect of mass flux ($T_{in} = 48.9$ C).

relationship between α and x, the wall temperature is read from the saturated boiling curves of Fig. 2.

The results of the boiling heat transfer predictions are compared to experimental data in Figs. 5(a) and (b). The comparison is made only in the fully detached bubble region since the present model is inapplicable elsewhere. It will be observed that the predictions are in reasonable agreement with the data. The effects of both mass velocity and subcooling are satisfactorily represented.

CONCLUSION

In summary, the data comparisons show that good predictions of subcooled swirl-flow CHF are obtained by using equation (12) with the parameters defined by equations (11), (16) and (32) with $\alpha_2 = 0.82$, $c = 1.5$ and $n = 0.9$. For quality flow, good CHF predictions are obtained using equation (8) with x_1 defined via equations (26), (28) and (29) and other parameters determined as for subcooled flow.

The presently proposed phenomenological model thus appears to provide a reasonable explanation for CHF at subcooled and low quality conditions in the presence of a twisted tape. The model is a natural extension of the CHF model previously developed for empty round tubes. With the exception of the modification of the empirical two-phase correction factor for the turbulent intensity, the modifications to the model have been simply those theoretically based changes needed to include the effects of swirling flow. The extension of the CHF model to boiling heat transfer in the detached bubble region, as proposed by Yang and Weisman [22], also appears to hold.

Acknowledgement—The authors appreciate the assistance of C. Qian in improving the prediction of empty-tube CHF data taken in the lower velocity region.

REFERENCES

1. F. Inasaka and H. Nariai, Evaluation of subcooled Critical Heat Flux correlations for tubes with and without internal twisted tapes, *Proceedings of 5th Int. Topical Meeting on Reactor Thermal Hydraulics*, Salt Lake City, Am. Nuc. Soc., LaGrange Park (1992).
2. J. Akoski, R. D. Watson, P. L., Goranson, A. Hassanian and J. Salmanson, Thermal hydraulic design issues and analysis for ITER diverter, *Fusion Technol.* **19,** 1729–1735 (1991).
3. J. Weisman and B. S. Pei, Prediction of Critical Heat Flux in flow boiling at low qualities, *Int. J. Heat Mass Transfer* **26,** 1463–1478 (1983).
4. J. Weisman and S. Illeslamlou, A phenomenological model for prediction of Critical Heat Flux under highly subcooled conditions, *Fusion Technol.* **13,** 654–659 (1988).
5. W. R. Gambill, R. D. Bundy and R. W. Wansbrough, Heat transfer, burnout and pressure drop for water in swirl flow through tubes with twisted tapes, *Chem. Engng Progress Symposium Series* **57**(32), 127–137 (1961).
6. R. Drizius, R. Skema and A. Slanciauskas, Boiling crisis in swirled flow of water in pipes, *Heat Transfer—Sov. Res.* **10**(4), 1–12 (1978).
7. A. Rosuel and G. Sourioux, Influence de tourbillions induits dans l'eau bouillante a la pression atmospherique sur les flux de calefaction, EURATOM Report No 5, S.N.E.C.M.A., Div. Atomique (1961).
8. F. Inasaka, H. Nariai, W. Fujisaki and H. Ishiguro, Critical Heat Flux of subcooled boiling in tubes with twisted internal tape, *Proceedings of ASME/JSME Thermal Eng. Conf., Reno, NV.* ASME, New York (1991).
9. S. T. Yin, A. Cardella, A. H. Abdelmessih, Z. Jin and B. P. Bromley, Assessment of heat transfer correlations package for water-cooled plasma facing components in fusion reactors, *Proceedings of 5th Int. Topical Meeting on Reactor Thermal Hydraulics (NURETH-V)*, Salt Lake City. Am. Nuc. Soc., LaGrange Park (1992).
10. J. A. Koski and C. D. Croessmann, Critical Heat Flux investigations for fusion-relevant conditions with the use of a rastered electron beam apparatus, ASME Paper 80-WA/NE-3 (1988).
11. B. Matzner, E. O. Moeck, J. E. Casterline and G. A. Wikhammer, Critical Heat Flux in long tubes at 1000 psi with and without swirl promoters, ASME Paper No. 65 WA/HT-30 (1965).
12. R. Brevi, M. Cumo, A. Palmieri and D. Pitimada, Forced convection heat transfer and burnout measurements with twisted-tapes, *La Termotecnica* **26,** 619–625 (1971).
13. F. W. Staub, Two-phase fluid modeling—The Critical Heat Flux, *Nucl. Sci. Engng* **35,** 190–199 (1963).
14. E. V. Moeck, G. A. Wikhammer, I. P. L. MacDonald and J. G. Collier, Two methods of improving the dryout heat flux for high pressure steam/water flow, *AECL* Report No. 2109 (1964).
15. R. Viskanta, Critical Heat Flux for water in swirling flow, *Nucl. Sci. Engng* **10,** 202–203 (1961).
16. D. Henkel, F. Mayinger, O. Schad and E. Weiss, Untersuchung der Kritischen Heizflaechenblastung bei Seidendem Wasser, *M.A.N.* Report No. 09.02.07, Maschienfabrik Augsburg-Nuremberg, Nuremburg, Germany (1964).
17. W. R. Gambill and R. D. Bundy, High heat transfer characteristics of pure ethylene glycol in axial and swirl flow, *A.I.Ch.E. Jl* **9,** 55–59 (1963).
18. J. Schlosser, A. Cardella, P. Massman, P. Chappius, H. D. Falter, P. Deschamps and G. H. Deschamps, Thermal-hydraulic tests on net diverter targets using swirl tubes, *Seventh Proceedings of Nuclear Thermal Hydraulics*, ANS Winter Meeting (1991).
19. J. A. Koski, Thermal-hydraulic considerations in the surface contouring of a limiter head for tore supra, *7th Proceedings of Nuclear Thermal Hydraulics*, ANS Winter Meeting (1991).
20. M. K. Jensen, A correlation for predicting the Critical Heat Flux condition with twisted tape swirl generators, *Int. J. Heat Mass Transfer* **27,** 2171–2173 (1984).
21. T. Crawford, C. B. Weinberger and J. Weisman, Two phase flow patterns and void fractions in downward flow, Part I, *Int. J. Multiphase Flow* **11,** 761–782 (1985).
22. J. Y. Yang and J. Weisman, A phenomenological model of subcooled flow boiling in the detached bubble region, *Int. J. Multiphase Flow* **17,** 77–94 (1991).
23. J. Y. Yang, Heat transfer rates and critical heat flux under subcooled boiling conditions, Ph.D. Thesis, University of Cincinnati, Cincinnati, OH (1990).
24. W. M. Rohsenow, A method of correlating heat transfer data for surface boiling of liquids, *Trans. ASME* **74,** 969–976 (1955).
25. S. Ying and J. Weisman, Prediction of Critical Heat Flux in flow boiling at intermediate qualities, *Int. J. Heat Mass Transfer* **29,** 1639–1648 (1986).
26. Y. L. Wong, D. C. Groenveld and C. Chen, CHF predictions for horizontal tubes, *Int. J. Multiphase Flow* **16,** 123–138 (1990).
27. J. Weisman, D. Duncan, J. Gibson and T. Crawford,

Effects of fluid properties and pipe diameter on two-phase flow patterns in horizontal lines, *Int. J. Multiphase Flow* **5**, 417–462 (1979).
28. S. Levy, Forced convection subcooled boiling—Prediction of vapor volumetric fraction, *Int. J. Heat Mass Transfer* **10**, 951–965 (1967).
29. R. Manglik and A. E. Bergles, Heat transfer and pressure drop correlations for twisted tape inserts part II. ASME Paper, HTD—Vol. 202, Enhanced Heat Transfer. ASME, New York, NY (1992).
30. A. Hussain, W. G. Choe and J. Weisman, Applicability of the homogeneous flow model to two-phase pressure drop in straight pipe and across area changes, *Chem. Engng Progress Symposium Series* **174**(74), 205–214 (1978).
31. J. O. Hinze, Fundamentals of the hydrodynamic mechanism of splitting and dispersion processes, *A.I.Ch.E. Jl* **1**, 189–197 (1955).
32. J. Weisman and L. Du, Computation of effect of heat addition on interfacial shear in bubbly flow, *Int. J. Multiphase Flow* **18**, 623–631 (1992).
33. J. Laufer, The structure of turbulence in fully developed pipe flow, NACA Technical Note No. 2954 (1953).